Tribological Qualification and Prediction of Fracture Probability of High-Performance Ceramics for Application in Flat Sliding Valves

The institute for Materials Applications (IWM)/DE and the Institute for Fluid Power Drives and Systems (ifas)/DE at RWTH Aachen University/DE are working on an industrial project "Proof of the Functionality of a Flat Sliding Valve with Ceramic Components".

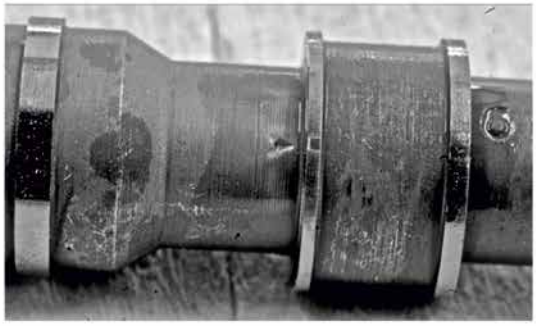

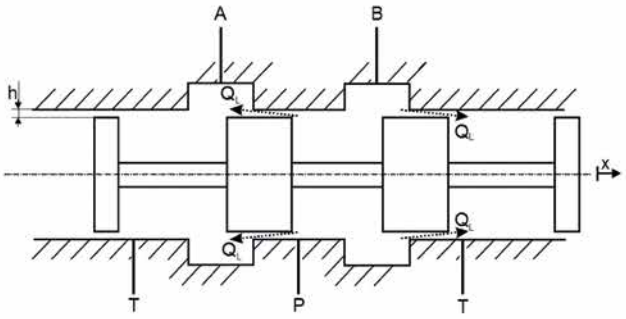

Fig. 1
Erosion, wear (l.) [1] and leakage (r.) of metallic spool valves

Introduction

For the control of fluid flows, valve-controlled systems with directional control valves are preferably used in hydraulic systems. In particular piston sliding valves, which consist essentially of cylindrical components, are primarily used. In this case, a rotationally symmetrical spool moves in the axial direction relative to the valve housing or to a sleeve. As a result, one or more flow cross sections can be created. Through these openings, the volume flow can be connected or disconnected to the corresponding working ports. In conventional sliding valves, spool and sleeve/housing are made of metallic materials. When using metallic spool valves, two weak points frequently occur in practice. The first weakness is shown in Fig. 1 where erosion and wear occur at the spool edges, which leads to a rounding of the control edges. The second weakness, the principle gap between the spool and sleeve/housing, which is necessary for adjusting the spool, leads to an annular gap with a height h of about 3–10 µm. The annular gap results in an unavoidable leakage between the chambers when a pressure differential is applied, as also shown in Fig. 1. The leakage results in a reduction of efficiency [1].

The use of a new innovative valve as shown in Fig. 2, which is part of this study, should lead to a reduction of the mentioned weak points. The valve is designed as a flat sliding valve with high-performance ceramic components, which have a number of advantages that can considerably improve the performance of valves. Compared to metallic materials, high-performance ceramics have significantly higher hardness and wear resistance. Therefore, the spool edge rounding by erosive wear, as it frequently occurs when steel is used, can be remarkably reduced. Moreover, the high possible parallelism of the ceramic plates allows almost closed gaps. Last but not

Keywords
flat sliding valve, fracture probability

C. Liu[1], S. Aengenheister[2], S. Herzog[1], Y. Deng[1], A. Kaletsch[1], A. Bezold[1], K. Schmitz[2], C. Broeckmann[1]
[1] IWM, RWTH-Aachen, 52062 Aachen
[2] ifas, RWTH-Aachen, 52074 Aachen
Germany

Corresponding author: C. Liu
E-mail: c.liu@iwm.rwth-aachen.de

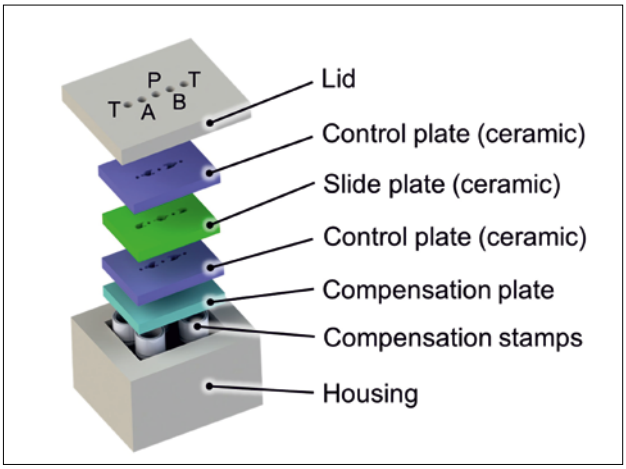

Fig. 2
Construction of the flat sliding valve

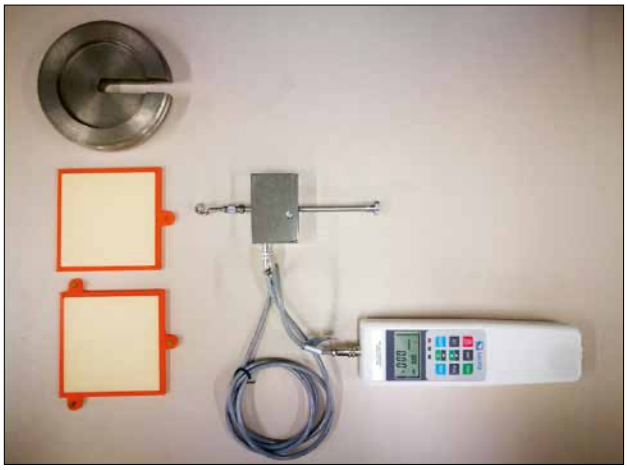

Fig. 3
Test set-up of static friction coefficient

least, the geometries are simple enough to be manufactured inexpensively from a ceramic pre-product with sufficient accuracy by laser cutting.

Tribological qualification

Three kinds of high-performance ceramics are under investigation in this study. They are isostatic-pressed aluminium oxide (Degussit AL23) supplied by Friatec AG/DE, sintered silicon carbide and hot-pressed silicon nitride supplied by FCT GmbH/DE. For convenience, the chemical symbols Al_2O_3, SiC and Si_3N_4 are used in the following text to represent the above mentioned ceramics, respectively.

High frequency movement of flat sliding valves requires a small friction coefficient in order to reduce wear and improve the dynamic performance. Therefore, a test workbench shown in Fig. 3 was developed by IWM and ifas at RWTH Aachen University to measure the static friction coefficient of the pairs of high-performance ceramic plates, which have a dimension of 100 mm × 100 mm × 4 mm. Since large inclinations of the workbench would result in inaccurate measurement of the traction force, a test table of a good levelness and negligible inclination was chosen. The 3D-printed plastic frames enclose the ceramic plates, which are stacked against each other. The bottom frame was used to fix the ceramic plate below and the upper frame with a side-attached eyelet was connected to the hook of the dynamometer sensor. The dynamometer can measure forces ranging from 0–50 N with a resolution of 0,01 N. Moreover, it is capable of recording force values with a frequency of 20 Hz. The data were then exported to the laptop as an excel file by a Matlab script. Since the realistic operation condition of a flat sliding valve is complex and the contact pressure between two ceramic plates is not constant, a mass set of 2–8 kg was used as the different normal weights for the plates. The ratio of the maximum traction and the weight yields the static friction coefficient.

In this work, the hydraulic oils HLP 32 and HLP 46 were used because they are widely applied in hydraulic valves. The numbers 32 and 46 indicate the different kinematic viscosities [mm²/s] of the oil at a temperature of 40 °C. Moreover, in order to control the amount of the hydraulic oil between plate pairs, a pipette dropper was used in this work.

For each test, 10 drops of oil (0,3 ml) were dropped on the surface of the bottom ceramic plate and the 2 kg mass was then placed on the upper frame for 24 h to accelerate the spreading process. This is based on the assumption that 10 drops of hydraulic oil could be evenly and uniformly distributed between two plates after 24 h and the amount of oil is representative of the real working condition of flat sliding valves.

A specific example of the traction curve is shown in Fig. 4 where the SiC plates pair

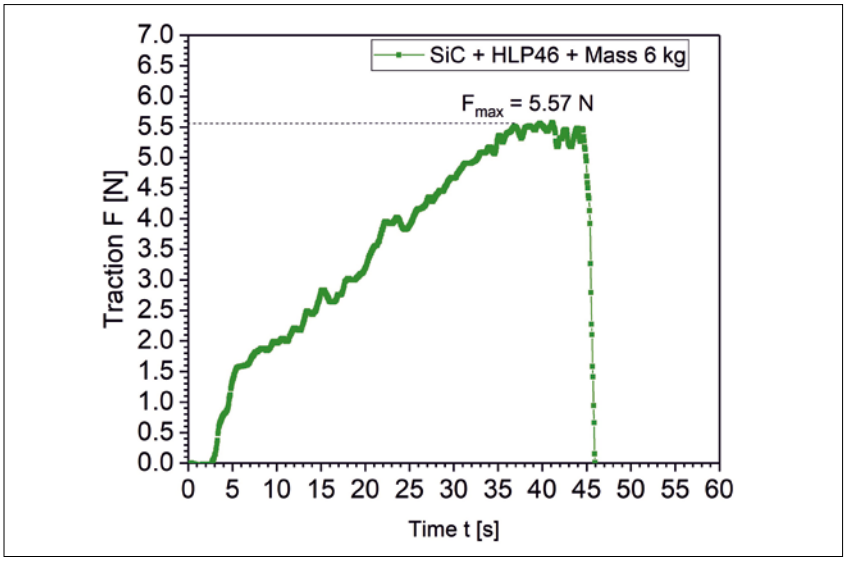

Fig. 4
An example of the traction curve

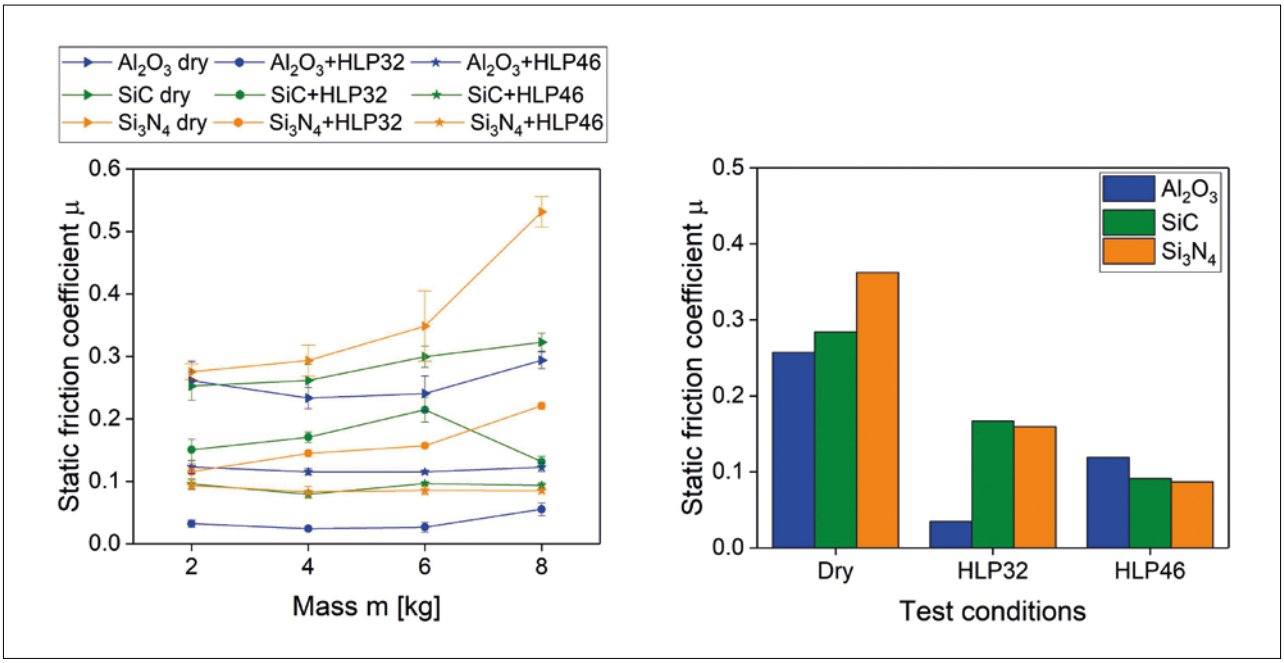

Fig. 5
Static friction coefficients with standard deviations of ceramic plates with different loading mass (l.), and the corresponding average values (r.)

with HLP 46 and a mass of 6 kg was studied. The traction increases almost linearly with test time and then comes to a plateau where it stagnates for several seconds. Any further increase in traction leads to the movement of upper plate. The maximum value of traction was used to calculate the static friction coefficient in this test.

The contact surfaces of all ceramic plates were polished with an average surface roughness R_a less than 0,05 µm and R_z below 1 µm. Three different ceramic pairs were studied: Al_2O_3–Al_2O_3, SiC–SiC and Si_3N_4–Si_3N_4. Three test conditions were investigated: dry without any medium, with HLP 32 and with HLP 46 as lubricants, respectively. For each scenario, the measurement was repeated five times. The static friction coefficients with their standard deviations of all scenarios with respect to different loading weights are shown in the left plot of Fig. 5. It is evident that in most cases the friction coefficient increases with a higher loading weight. This is due to the fact that the area of contact for the plate pairs is actually much smaller than the area of coverage. Because of microscopic irregularities in the surface, the plate is actually riding on a small fraction of the coverage area. Since such points of contact are deformable, an increase in normal force will increase the area of actual contact and increase the resistance against movement.

Moreover, the friction coefficients of all ceramic pairs were reduced significantly when the hydraulic oil was applied. This is easy to understand because hydraulic oil acts as a lubricant between the ceramic plates and the lubricant film will reduce the actual contact surface and resistance to movement. Furthermore, an interesting phenomenon could be observed from the left curves in Fig. 5. For SiC and Si_3N_4, HLP 46 reduces the friction coefficients to a higher extent than HLP 32. However, the situation of Al_2O_3 is quite opposite since HLP 32 reduces the friction considerably more than HLP 46. This phenomenon is more intuitively shown in the right part of Fig. 5, where the friction coefficients of different loading weights were averaged.

While a reasonable explanation for this phenomenon is lacking, it gives a hint that when one selects Al_2O_3 as the best candidate, HLP 32 should be used in the flat sliding valve as lubricant, when SiC or Si_3N_4 are selected, HLP 46 should be used. A comparison of the static friction coefficients in the above measured scenarios yields the conclusion that the ceramic pair Al_2O_3–Al_2O_3 with hydraulic oil HLP 32 is the best combination for the flat slide valves from a tribological point of view.

Theory of fracture probability calculation

Compared with metallic materials, high-performance ceramics have numerous advantages such as generally lower density, significantly higher hardness, better wear and corrosion resistance which can significantly enhance the performance and life time of the flat sliding valves. However, high-performance ceramics have natural flaws, being induced during the manufacturing process and machining operations such as fabrication, grinding and polishing. These flaws scatter widely in size, location and orientation leading to a large scatter of the flexural strength and lifetime in different production batches. This indicates the data found in literature as well as in suppliers' data sheets can be used for reference only. Since it is not feasible to determine the size, location and orientation of each flaw with reasonable effort, a probabilistic approach is required to analyse the distribution of strength and fracture probability [2]. The most commonly method used for the strength characterisation and fracture probability calculation of high-performance ceramics is the

two-parameter Weibull approach, which is defined according to eq. (1):

$$P_f = 1 - \exp\left(-\left[\frac{\sigma(x,y,z)}{\sigma_0}\right]^m dV\right) \quad (1)$$

where $\sigma(x, y, z)$ is the non-uniform stress distribution of a component, m the Weibull modulus and σ_0 the characteristic strength, respectively. The Weibull modulus m describes the variation in the strength resulting from the distribution of flaws within the microstructure of ceramics. A low value of the Weibull modulus indicates a higher scatter of the flexural strength and hence lower reliability, while a high Weibull modulus indicates a more homogeneous flaw distribution throughout the entire volume and hence higher reliability. The characteristic strength σ_0 corresponds to strength value where 63,2 % of the test specimens would fail. m and σ_0 could be directly calculated based on the maximum likelihood estimator method after the bending test is completed.

However, σ_0 varies with different test specimen geometries and loses much of its practicability in the reliability analysis and fracture probability calculation of high-performance ceramic components. Therefore, another form of the two-parameter Weibull approach is more widely used. This form is defined by eq. (2), provided that the statistically distributed flaws inside the volume are the reason for component failure [3]:

$$P_f = 1 - \exp\left(-\frac{1}{V_0}\int_V \left[\frac{\sigma(x,y,z)}{\sigma_{0V}}\right]^m dV\right) \quad (2)$$

where V_0 is the unit volume and σ_{0V} is the Weibull scale parameter or normalised flexural strength, respectively. Unlike characteristic strength σ_0, the Weibull scale parameter σ_{0V} is a volume-independent and material-specific strength value and shows its significance.

In the FE-simulation, the fracture probability of each element is calculated first by eq. (3) and then the overall fracture probability of the structure can be obtained based on Weakest-link-theory by eq. (3, 4):

$$^{j)} = 1 - \exp\left(-\left[\frac{\sigma_1(x,y,z)}{\sigma_{0V}}\right]^m V^{(ij)}\right) \quad (3)$$

$$P_{f,tot} = 1 - \left[\prod_{i=1}^{NE}\prod_{j=1}^{NGE}\left(1 - P_f^{(ij)}\right)\right] \quad (4)$$

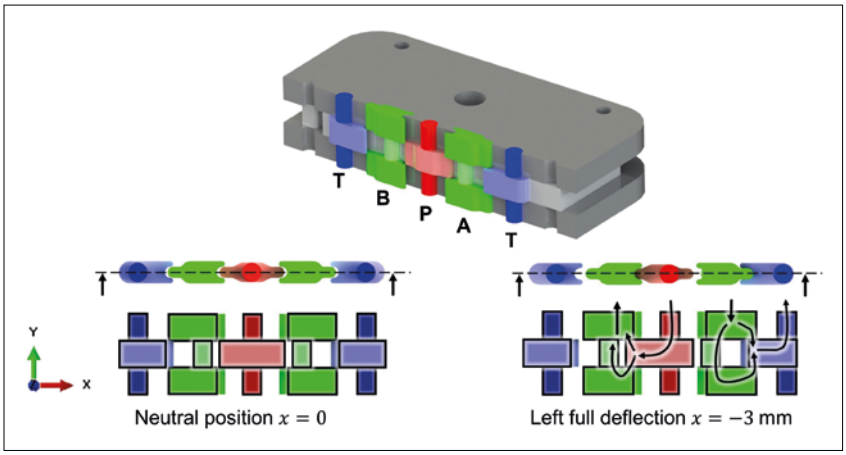

Fig. 6
Flow channels P, A, B and T (top) and flow cross sections, cutouts and flow directions (bottom)

where NE is the number of finite elements and NGE is the number of Gaussian integration points per element. $V^{(ij)}$ is the volume of the corresponding integration point volume.

CFD simulation

In order to calculate the fracture probability based on eq. (3) and eq. (4), the maximum principal stress distribution $\sigma_1(x, y, z)$ of the flat sliding valve must be obtained beforehand. However, during the operation of the flat sliding valve, the fluid flow behaviour is complex and the pressure distribution of the contact regions between the fluid flows and the ceramic plates is unknown. Therefore, the Computational Fluid Dynamics (CFD) simulation has been used to obtain the pressure profiles of contact regions in fluid flows.

A sectional view of the flat sliding valve is shown in Fig. 6 (top) where the channels inlet P, working ports A and B, and tank T which are marked in red, green and blue, representing the flow channels. During operation, the upper and bottom control plates are fixed and the middle slide plate moves left and right to change the connected ports. This is shown in Fig. 6 (bottom) where the flow cross sections, their corresponding cutouts and flow directions in two typical positions are illustrated. When the slider is in the neutral position where x = 0, the port P and port T is not connected to port A or B. In this position, all flow channels are separated from each other and no flow between the ports exists. When the slider moves to the left full deflection x = –3 mm, the port P is connected to port B and port A is connected to port T. Due to symmetry, the scenario of the right full deflection x = 3 mm can be analysed similarly.

It should be noted that when x equals 1 or –1 mm, the middle slider is in a vital position where the flat sliding valve is just opening or closing.

The CFD simulation was performed with the software Ansys Fluent. Fig. 7 shows the fluid flows in port P and port B at left full deflection where x = –3 mm. For the simulation a fluid with a constant density of 827,9 kg/m³ and a constant dynamic viscosity of 0,04 kg/(m s) was used, which corresponds to the HLP 46 at 40 °C.

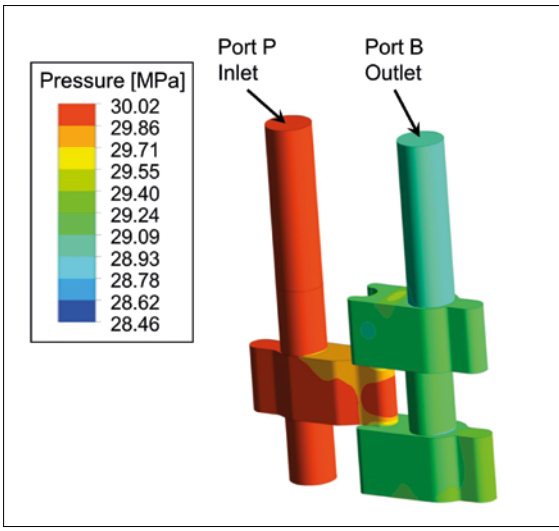

Fig. 7
Pressure distribution along the flow cross-section, at left full deflection

Tab. 1
Material properties used in FE-simulation and fracture probability calculation

Ceramics	Al_2O_3	SiC	Si_3N_4
Young's modulus E, [GPa]	380	400	310
Poisson ratio ν	0,22	0,15	0,26
Weibull modulus m	10	10	15
Flexural strength σ_{0V}, [MPa]	320	400	910

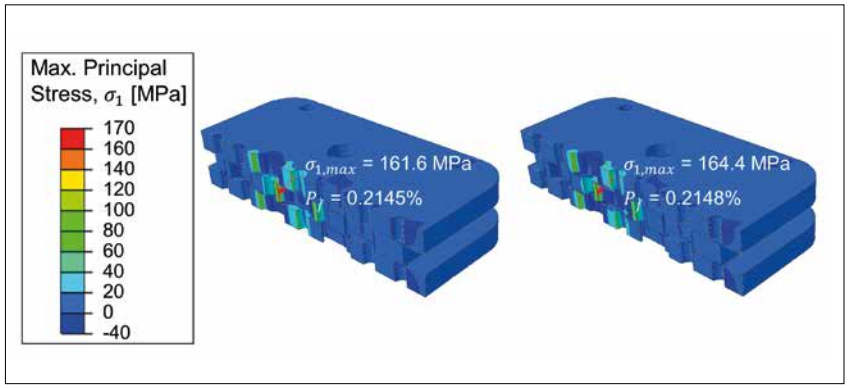

Fig. 8
Stress distribution of applying pressure from the CFD results (l.), and constant inner pressure of 300 bar (r.)

According to the requirements defined by the project-accompanying working group (VDMA/DE), the permissible pressure drop between the inlet and outlet port is 10 bar. With a pressure drop of 10 bar, the volume flow was calculated to be 30 l/min and was set as boundary condition at the inlet port P. The port B was defined as an outlet with a pressure of 290 bar, since the maximum working pressure is 300 bar. The static pressure distribution of the fluid flows at left full deflection is shown in Fig. 7. It is evident that the pressure distribution of the fluid flow is inhomogeneous and ranges from 290–300 bar. The pressure profiles of the fluid flows from the CFD simulation were later used as loading conditions for the Finite Element (FE) simulation for the ceramic plates in the flat sliding valves.

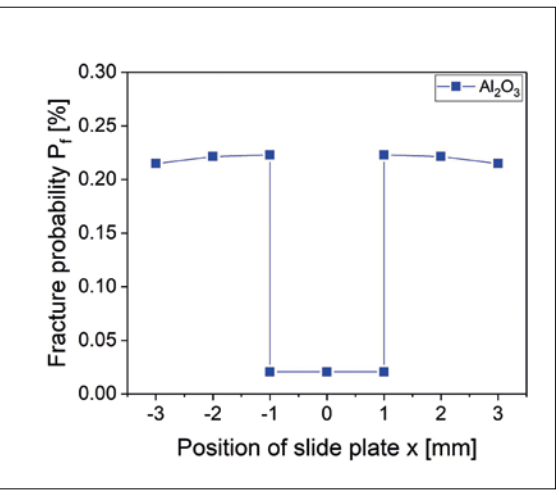

Fig. 9
The fracture probability of the flat sliding valve constructed with Al_2O_3

FE-Simulation and fracture probability calculation

The idea of applying the results from the CFD simulation into FE-simulation is attractive since the inhomogeneous pressure distribution of the fluid flows obtained from the CFD simulation represents the realistic scenario in service.

In the FE-simulation, the ceramics were defined as purely elastic materials in ABAQUS and their material properties were found from the suppliers' data sheet [4, 5] and are listed in Tab. 1.

As a case study, Al_2O_3 was investigated firstly. The upper and bottom control plates were fixed. The pressure distribution of the fluid flows from the CFD simulation was successfully transferred into the corresponding surfaces of the slide and control plates as surface loadings.

The maximum principal stress distribution at left full deflection (x = –3 mm) is shown in the left contour plot in Fig. 8. The right contour plot was obtained by applying the maximum working pressure of 300 bar uniformly distributed on the fluid and plates contact regions. Comparing the contour plots of both situations, the results show similar stress distribution, maximum principal stress value and fracture probability. More specifically, the peak principal stress and fracture probability of the situation with uniformly distributed pressure 300 bar is slightly higher than the case with CFD results. This indicates this simplification, which significantly reduces computational time, is relatively more conservative and could be further appropriately used in the simulations of different slider positions afterwards.

Three additional slider positions where x equals –2, –1 and 0 mm were studied. As mentioned before, x equals –1 mm is a vital position where the flat sliding valve is just opening or closing. When treated as close state, only the pressure in channel P was applied. When treated as open state, both the pressure in channel P and B were considered. Therefore, two fracture probabilities were calculated corresponding to the valve close and open state at position x = –1 mm.

The short-term fracture probability of Al_2O_3 flat sliding valves at different slider positions is shown in Fig. 9. From this figure we may conclude when the valve is in the close state, the fracture probability remains constant with a very small value of around 0,021 %. When the valve opens, the fracture probability increases significantly to around 0,22 % due to more contact regions and pressurized surfaces. The worst case is observed at position x = –1 mm when the valve is just opening. The worst case was further investigated for SiC and Si_3N_4. It can be seen from Tab. 2 that despite different Young's modulus and Poisson ratio of these high-performance ceramics, the peak maximum principal stresses of all ceramics are almost identical. Moreover, compared to Al_2O_3, Si_3N_4 has significantly higher flexural strength and the fracture probability drops considerably to nearly zero. This does not necessarily

Developing the Powder Metallurgy Future

european powder
metallurgy association

CELEBRATING 30 YEARS EPMA european powder metallurgy association

International Congress & Exhibition

13 – 16 October 2019

Maastricht Exhibition & Congress Centre (MECC),
Maastricht, The Netherlands

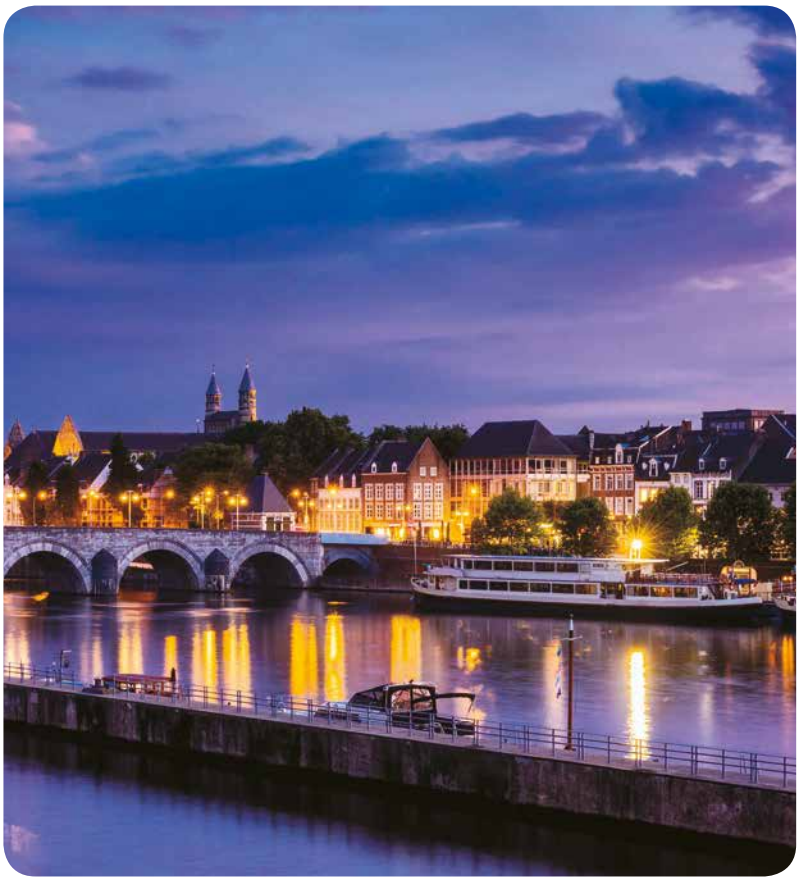

EURO PM2019 CONGRESS & EXHIBITION

www.europm2019.com

EURO PM2019 CONGRESS & EXHIBITION

Tab. 2
The peak value of the maximum principle stress and fracture probability of Al_2O_3, SiC and Si_3N_4 in the worst case (300 bar loading, valve position at x = –1 mm just opening)

Ceramics	Al_2O_3	SiC	Si_3N_4
Peak stress, $\sigma_{(1, max)}$, [MPa]	161,92	161,07	162,84
Fracture probability P_f [%]	0,223	0,023	$5{,}46 \cdot 10^{-10}$

mean Si_3N_4 is the best choice for valves, because choosing the most appropriate high-performance ceramic needs a more comprehensive and full-scale investigation of the mechanical properties and their costs. Since the microstructure and edge quality decide the materials' macroscopic properties, the microstructures and processability by laser-cutting of these high-performance ceramics will be studied in the next phase of this project.

Summary

In this work, the static frictional coefficients of Al_2O_3–Al_2O_3, SiC-SiC and Si_3N_4–Si_3N_4 plate pairs with different loading masses were measured via a workbench developed by IWM and ifas at RWTH Aachen University. The results show that the polished Al_2O_3–Al_2O_3 pair has the lowest static frictional coefficients in dry condition. Moreover, the influence of two hydraulic oils on the friction was studied. While HLP 32 hydraulic oil reduces the frictional coefficients of Al_2O_3–Al_2O_3 pair to a significantly higher extent than HLP 46, the opposite situation was observed for SiC–SiC and Si_3N_4–Si_3N_4 where HLP 46 works better. This indicates when Al_2O_3 is selected in the hydraulic system, the hydraulic oil HLP 32 is a good choice and when SiC or Si_3N_4 is selected, HLP 46 is better for flat sliding valve in terms of tribological performance.

Furthermore, the CFD simulation was carried out to obtain the pressure profiles of the fluid flows on the contact regions. These pressure profiles from the CFD simulation were transferred to the corresponding areas of ceramic plates in the FE-simulation as surface loadings. The maximum principal stress distribution of the ceramic plates was then obtained in the FE-simulation and compared to the situation where the constant inner pressure was applied. With the information of the stress distribution of control and slide plates in flat sliding valves, the fracture probability was calculated based on the Weibull approach and weakest-link-theory. It was found that ceramic plates have the highest fracture probability at vital position when the flat sliding valve is just opening, which was seen as the worst case. The fracture probabilities of all three ceramics in the worst case situation were calculated and Si_3N_4 has a negligible fracture probability. However, determining the most appropriate ceramic material for the flat sliding valve needs a deeper insight into the microstructure and edge quality of the laser cut openings in the high-performance ceramic slide plates.

Acknowledgement

This project was funded by the German Federation of Industrial Research Associations (AiF) under the contract number IGF-19576. Authors take this opportunity to say thank you to Friatec AG/DE and FCT GmbH/DE for the preparation of the ceramic plates.

References

[1] Schumacher, J.T.: Alterungs- und Verschleißverhalten von Druckübertragungsmedien und hydraulischen Ventilen. Aachen 2014

[2] Bezold, A.; Pfaff, E.; Broeckmann, C.: Product and system innovation based on integrative design with ceramic (IDC): Reliability analysis. Ceramic Applications 2 (2014) [2] 54–58

[3] Munz, D.; Fett, T.: Ceramics: Mechanical properties, failure behaviour, materials selection. Berlin, Heidelberg 1999

[4] FCT GmbH, Werkstoffvergleich Keramik / Metall. [Online] Available: https://www.fcti.de/de/werkstoffdatenbank/index.php

[5] Friatec AG, Werkstoffdatenblatt. [Online] Available: https://www.friatec.de/content/friatec/de/Keramik/FRIALIT-DEGUSSIT-Oxidkeramik/Technische-Keramik/downloads/WD_FRIALIT-AL23.pdf